

# Measurement of Nonlinear Mode Couplings in the Large Mirror Device-Upgrade

Takuma YAMADA, Sanae –I. ITOH<sup>1)</sup>, Shigeru INAGAKI<sup>1)</sup>, Yoshihiko NAGASHIMA, Shunjiro SHINOHARA<sup>2)</sup>, Takashi MARUTA<sup>2)</sup>, Kenichiro TERASAKA<sup>2)</sup>, Kunihiro KAMATAKI<sup>2)</sup>, Naohiro KASUYA<sup>3)</sup>, Masatoshi YAGI<sup>1)</sup>, Yoshinobu KAWAI<sup>1)</sup>, Akihide FUJISAWA<sup>3)</sup> and Kimitaka ITOH<sup>3)</sup>

*Graduate School of Frontier Sciences, The University of Tokyo, Kashiwa 277-8561, Japan*

<sup>1)</sup>*Research Institute for Applied Mechanics, Kyushu University, Kasuga 816-8580, Japan*

<sup>2)</sup>*Interdisciplinary Graduate School of Engineering Sciences, Kyushu University, Kasuga 816-8580, Japan*

<sup>3)</sup>*National Institute for Fusion Science, Toki 509-5292, Japan*

(Received: 1 September 2008 / Accepted: 10 December 2008)

Experimental study of plasma turbulence has been proving theoretical predictions by using multi-channel diagnostics and analyzing techniques such as bi-spectral analysis. We performed a fluctuation measurement of the ion saturation-current with a 64-channel poloidal Langmuir probe array in the Large Mirror Device-Upgrade. A number of fluctuation peaks in the poloidal wave number–frequency space were observed, and they satisfied the matching conditions of wave number and frequency with each other. The nonlinear mode couplings among the fluctuation peaks were confirmed by two-dimensional bi-coherence analysis. By amplitude correlation technique, three original parent modes were found. All the other fluctuation peaks were quasi-modes, which were successively generated by mode couplings from the three original parent modes.

Keywords: linear plasma, drift wave, turbulence, bi-coherence, amplitude correlation technique

## 1. Introduction

Theoretical studies and simulations on drift wave turbulence predict interesting models that the drift waves are strongly coupled with meso-scale waves such as zonal flows and streamers, which have strong influences on transport rates [1]. Recent progress on measurement methods such as multi-channel measurements [2–5], and analyzing techniques such as bi-spectral analysis [6, 7] make it possible to observe these meso-scale structures in plasmas. For example, zonal flow was measured in the Compact Helical System plasma [8], and streamer was measured in the Large Mirror Device-Upgrade (LMD-U) linear plasma [9]. Experimental study has been proving theories and becoming more important for investigating plasma turbulence to contribute to the ITER project.

In order to study the nonlinear mode couplings and meso-scale structures in drift wave turbulence experimentally, multi-probe measurements were performed in the LMD-U linear plasma. The LMD-U plasma allows multi-channel Langmuir probe measurement because of its low temperature. With the multi-channel measurement, many interesting features of plasma turbulence have been observed in LMD-U. For example, drift wave modes [10], route to drift wave turbulence [11], and broadband mode [12] were observed. With a 64-channel poloidal Langmuir probe [13], two-dimensional (2D) power spectrum of the ion saturation-current fluctuation, which showed a number of fluctuation peaks in the poloidal wave number–frequency space, was observed.

The poloidal wave numbers and frequencies of the fluctuation peaks satisfied the matching condition with each other and suggested that these peaks were produced successively by nonlinear mode couplings from three irreducible parent modes [14]. The mode couplings among the fluctuation peaks were confirmed by bi-spectral analysis with considering only the matching condition in the frequency space [11]. The results from 2D bi-spectral analysis, which was considering the matching conditions of the poloidal wave number and frequency, was introduced [9].

In this paper, we present the results from the 2D bi-spectral analysis and investigation of the energy transfer direction in detail. The successive generation of the quasi-modes from the original parent modes is visualized.

## 2. 2D Bi-coherence Analysis

Bi-spectral analysis [6] examines the relationship among three waves with wave numbers and frequencies of  $(\mathbf{k}_1, \omega_1)$ ,  $(\mathbf{k}_2, \omega_2)$  and  $(\mathbf{k}_3, \omega_3)$ , which satisfy the matching conditions  $\mathbf{k}_3 = \mathbf{k}_1 + \mathbf{k}_2$  and  $\omega_3 = \omega_1 + \omega_2$ . By using a poloidal probe array, the matching conditions of not only the frequency  $\omega$ , but also the poloidal wave number  $k_\theta$  can be considered. A poloidal probe array can measure the poloidal mode number  $m$  of the fluctuation wave ( $m$  is an integer), which is related to the poloidal wave number  $k_\theta$  by  $m = r_p k_\theta$ , where  $r_p$  is the radius of the probe array.

When the Fourier transformed expression of a 2D waveform  $z(\theta, t)$  is  $Z(m, f)$ , where  $\theta$  is the poloidal angle of the probe and  $f = \omega/2\pi$ , the bi-spectrum  $B$  of the three waves is expressed as  $B = \langle Z(m_1, f_1)Z(m_2, f_2)Z^*(m_3, f_3) \rangle$ . When the three waves fluctuate independently, the absolute

author's e-mail: takuma@k.u-tokyo.ac.jp

value  $|B|$  becomes 0. When the phases of the three waves are connected by a certain relationship,  $|B|$  becomes finite. The bi-coherence  $b$ , which is a normalized value of  $B$ , and the bi-phase  $\phi_b$ , which shows the relationship among the phases of the three waves, are expressed as

$$b^2 = \frac{|B|^2}{\langle |Z(m_1, f_1)Z(m_2, f_2)|^2 \rangle \langle |Z(m_3, f_3)|^2 \rangle},$$

$$\phi_b = \tan^{-1} \frac{\text{Im}(B)}{\text{Re}(B)}, \quad (1)$$

respectively. Bi-coherence analysis is important for investigating the coupling among three waves. When the bi-coherence  $b$  is finite for the three waves, it suggests that one wave is produced by nonlinear mode coupling of the other two waves.

2D bi-spectral analysis is effective when the plasma turbulence has many fluctuation peaks in the  $m$ - $f$  plane. The mode couplings among the waves become clearer by decomposing the bi-coherence analysis into the  $m$  plane.

### 3. Spectral Analysis in LMD-U

The LMD-U [10] vacuum vessel has the axial length of 3740 mm, with a straight axial magnetic field (0.01–0.15 T). The LMD-U plasma has the plasma radius of about 50 mm, since the plasma is generated by radio-frequency wave (7 MHz / 3 kW) inside a quartz tube with an inner diameter of 95 mm. The quartz tube is filled with argon gas with a pressure of 0.2–0.8 Pa. The electron density and temperature of the plasma are about  $10^{19} \text{ m}^{-3}$  and 3 eV, respectively. Resistive drift wave mode is excited in the LMD-U plasma by its density gradient. By increasing the magnetic field (over 0.04 T) or decreasing the argon pressure (under 0.4 Pa), the excited mode changes into drift wave turbulence [12]. A 64-channel poloidal Langmuir probe array [13] at  $r_p = 40$  mm is installed on LMD-U.

The 2D waveform  $z(\theta, t)$  of the ion saturation-current fluctuation generated in LMD-U was measured with the 64-channel poloidal probe array. The sampling frequency was 1 MHz. In the discharge conditions of the magnetic field of 0.02 T and the argon pressure of 0.27 Pa, the 2D power spectrum  $S(m, f) = |Z(m, f)|^2$  showed a single drift wave mode with  $(m, f) = (3, 4.2 \text{ kHz})$ . In this paper,  $m \geq 0$ , and positive  $f$  indicates the propagation in the electron diamagnetic direction. By increasing the magnetic field to 0.09 T,  $z(\theta, t)$  changed into drift wave turbulence. In this case,  $S(m, f)$  showed a number of fluctuation peaks in the  $m$ - $f$  plane (see Fig. 1). The small extension of the mode numbers of the fluctuation peaks is caused by the misalignment of the probe tips, which was discussed in Ref. [13]. (In addition, broadband fluctuation with the same decay laws in the  $m$  and  $f$  space was also observed [12].)

According to Fig. 1, the  $(m, f)$  of the fluctuation peaks are (A: 1, 2.8 kHz), (B: 2, 3.2 kHz), (C: 1, -0.9 kHz), (D: 2, 5.6 kHz), (E: 2, 1.9 kHz), (F: 1, 4.1 kHz), (G: 3, 8.4 kHz), (H: 3, 4.7 kHz), (I: 2, 6.9 kHz) and

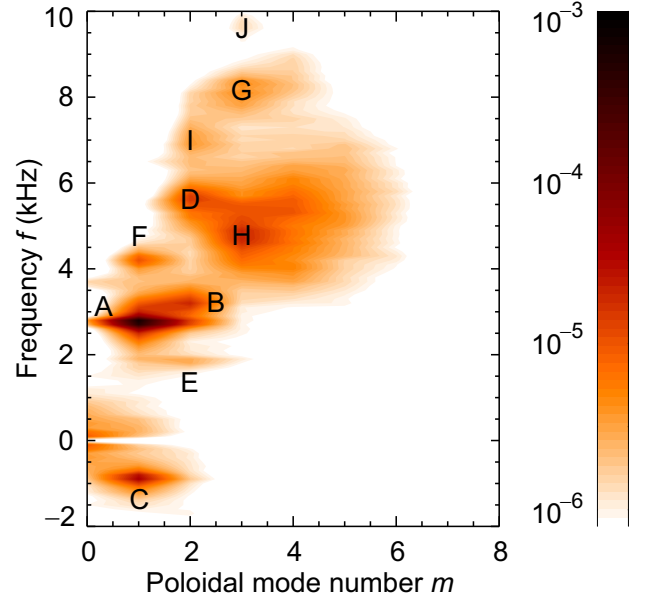


Fig. 1 Contour plot (arb. unit) of 2D power spectrum of ion saturation-current fluctuation in LMD-U. The discharge conditions (magnetic field, argon pressure) are (0.09 T, 0.27 Pa). Positive  $f$  indicates the propagation in the electron diamagnetic direction. The frequency resolution is 0.1 kHz. A number of fluctuation peaks, which satisfy the matching conditions with each other, are observed.

(J: 3, 9.7 kHz). Examining the mode numbers and frequencies of the fluctuation peaks, we can find out that these fluctuation peaks satisfy the matching condition with each other. For example, the peaks (D) and (G) are the higher harmonics of the peak (A), i.e., ( $\alpha$ :  $D = A + A$ ) and ( $\beta$ :  $G = A + D$ ). Other matching conditions are ( $\gamma$ :  $E = A + C$ ), ( $\delta$ :  $B = C + F$ ), ( $\epsilon$ :  $H = C + D$ ), ( $\zeta$ :  $H = A + E$ ), ( $\eta$ :  $I = A + F$ ) and ( $\kappa$ :  $J = A + I$ ). The Greek letter is the label of each mode coupling.

When the matching condition exists, there is a possibility that the three waves are nonlinearly coupled, and one wave is forced to be excited by the other two waves. The wave excited in this way is called quasi-mode [15]. By this argument, we can suspect that many of the fluctuation peaks are quasi-modes, which are excited by the origin of three irreducible real modes. The combination of the three original parent modes is considered to be (A, B, C) or (A, C, F), for example. The mode coupling of the waves is verified by bi-coherence analysis, and the energy transfer direction from parent mode to child mode is estimated by amplitude correlation technique.

### 4. Mode Couplings and Energy Transfer

To evaluate the mode couplings expected above, bi-coherence analysis was applied to the ion saturation-current fluctuation. The 2D Fourier transformed expression  $Z(m, f)$  was calculated first, and  $m_1, f_1, m_2$  and  $f_2$  were chosen to investigate the bi-coherence  $b$  among the

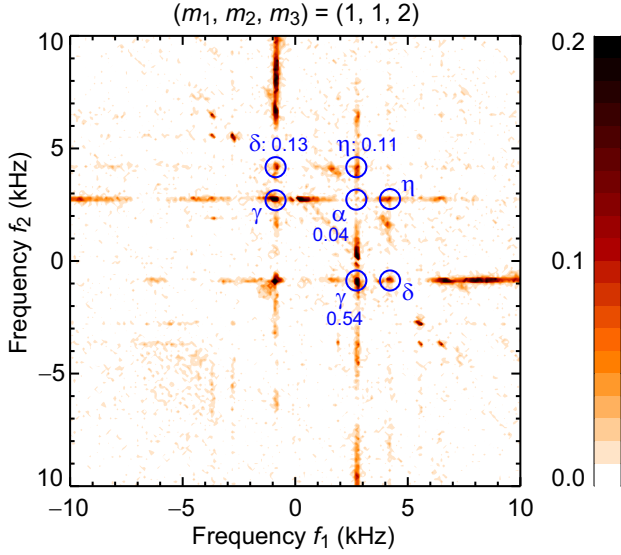


Fig. 2 Contour plot of squared bi-coherence among three waves  $(m_1, f_1)$ ,  $(m_2, f_2)$  and  $(m_3, f_3)$ , which satisfy the matching condition  $(m_1, m_2, m_3) = (1, 1, 2)$ . Frequency ranges are  $(-10 \text{ kHz} \leq f_1, f_2 \leq 10 \text{ kHz})$  and  $(-20 \text{ kHz} \leq f_3 \leq 20 \text{ kHz})$ . Circles indicate the mode couplings  $\alpha$ ,  $\gamma$ ,  $\delta$  and  $\eta$ . Values are the squared bi-coherence  $b^2$ .

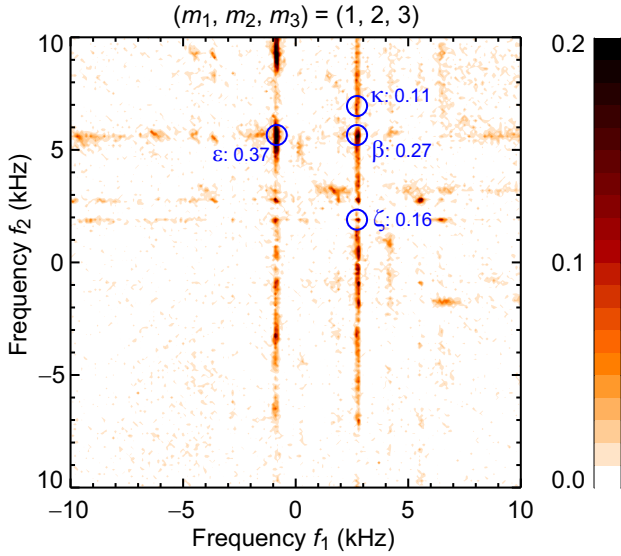


Fig. 3 Contour plot of squared bi-coherence among three waves  $(m_1, f_1)$ ,  $(m_2, f_2)$  and  $(m_3, f_3)$ , which satisfy the matching condition  $(m_1, m_2, m_3) = (1, 2, 3)$ . Frequency ranges are the same as Fig. 2. Circles indicate the mode couplings  $\beta$ ,  $\epsilon$ ,  $\zeta$  and  $\kappa$ . Values are the squared bi-coherence  $b^2$ .

three waves  $(m_1, f_1)$ ,  $(m_2, f_2)$  and  $(m_3 = m_1 + m_2, f_3 = f_1 + f_2)$ . Figure 2 shows an example of the bi-coherence analysis applied to  $Z(m, f)$ . In this figure,  $m_1$  is fixed to 1 and  $m_2$  is fixed to 1 (therefore,  $m_3 = 2$ ). The horizontal and vertical axes are  $f_1$  and  $f_2$ , respectively. Thus, the squared bi-coherence  $b^2$  in the case of  $(m_1, m_2, m_3) = (1, 1, 2)$  in the range of  $(-10 \text{ kHz} \leq f_1, f_2 \leq 10 \text{ kHz})$  and  $(-20 \text{ kHz} \leq f_3 \leq 20 \text{ kHz})$  is plotted in this figure. The result

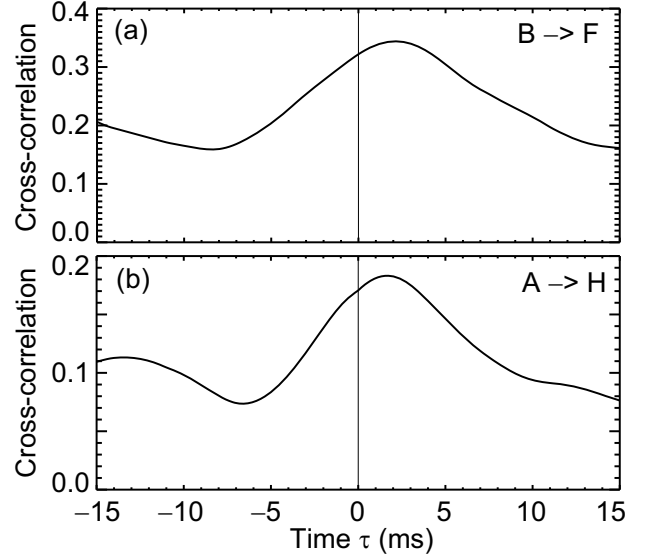


Fig. 4 Cross correlation functions between time evolutions of wave powers; (a)  $C_{BF}(\tau)$  and (b)  $C_{AH}(\tau)$ .  $\tau$  of the peaks indicate time delays of (a) (F) from (B) and (b) (H) from (A). They are ensembles of ten discharges.

is an ensemble of 300 time windows (each time window is 10 ms long), so that the confidence level is 0.003 ( $= 1/300$ ). Self-nonlinear coupling of ( $\alpha$ :  $D = A + A$ ), which is shown at  $f_1 = f_2 = 2.8 \text{ kHz}$ , is weak ( $b^2 = 0.04$ ) but above the confidence level. Other combinations of the mode couplings can be confirmed in Fig. 2. The values of the squared bi-coherence  $b^2$  are ( $\gamma$ :  $E = A + C$ : 0.54), ( $\delta$ :  $B = C + F$ : 0.13) and ( $\eta$ :  $I = A + F$ : 0.11). Figure 3 shows the squared bi-coherence in the case of  $(m_1, m_2, m_3) = (1, 2, 3)$ . The mode couplings among waves with  $m = 1, 2$  and 3 are clarified. The values of the squared bi-coherence  $b^2$  are ( $\beta$ :  $G = A + D$ : 0.27), ( $\epsilon$ :  $H = C + D$ : 0.37), ( $\zeta$ :  $H = A + E$ : 0.16) and ( $\kappa$ :  $J = A + I$ : 0.11). Thus, the expected mode couplings were confirmed and it was proved that the number of the irreducible parent modes was three.

Bi-coherence analysis indicates only the existence of the mode coupling among three waves. The quasi-mode which is generated by the mode coupling of the other two modes is not determined by bi-coherence analysis. Therefore, the three original parent modes are not clarified yet. The powers of the fluctuation peaks (A) and (C) are relatively strong and stable in time, while other peaks appears intermittently with short lifetimes. The correlation lengths of (A) and (C) in the poloidal direction are long and they are produced globally in the poloidal direction [12]. From these facts, it is natural to conclude that (A) and (C) are the original parent modes. The left problem is whether the third parent mode is. (B) and (F) are the candidates.

To explore the parent mode between two modes, the energy transfer direction is required. Amplitude correlation technique [16, 17] can support to find the direction. This technique is effective when the amplitude of the

waves fluctuate with time. Time evolutions of the powers of two waves  $S_1(t) = S(m_1, f_1, t)$  and  $S_2(t) = S(m_2, f_2, t)$  are calculated by short-time Fourier transformation, and the cross-correlation function between  $S_1(t)$  and  $S_2(t)$  are evaluated as

$$C_{12}(\tau) = \frac{\langle [S_1(t) - \bar{S}_1][S_2(t + \tau) - \bar{S}_2] \rangle}{\sqrt{\langle [S_1(t) - \bar{S}_1]^2 \rangle \langle [S_2(t) - \bar{S}_2]^2 \rangle}}. \quad (2)$$

When the two waves fluctuate similarly in time, a peak in the cross-correlation function appears near  $\tau = 0$  and the time of the peak indicates the response of  $S_2(t)$  to  $S_1(t)$ . Figure 4(a) shows the cross-correlation function  $C_{BF}(\tau)$  between the time evolutions of the powers of (B) and (F) (time window is 10 ms and move step is 0.2 ms). The peak of  $C_{BF}(\tau)$  is seen at  $\tau = 2$  ms, which indicates that (F) responds in 2 ms after the variation of (B). This delay time means the typical duration which is needed to complete the energy transfer from (B) to (F). Therefore, (B) is considered to be the parent mode of (F). The matching condition can be rewritten as  $(F = B - C)$ . Figure 4(b) shows another example; the cross-correlation function  $C_{AH}(\tau)$ . It has a peak at  $\tau = 1.6$  ms. Therefore, (H) responds in 1.6 ms after (A), and (A) must be the parent mode of (H).

By these analyses, the three original parent modes are considered to be (A, B, C). All the other waves (F–J) are quasi-modes, which are successively generated by mode couplings from the original parent modes (A, B, C). (A) and (B) have the features of drift wave [10], while (C) is not a drift wave since its intensity is strong at the plasma edge region and weak at the steep density gradient region [11]. Figure 5 is a summarized chart of the provided results. The figure visually shows the successive generation of the quasi-modes from the original parent modes. (A, B, C) are the original parent modes, (D, E, F) are the quasi-modes of the first generation, (G, H, I) are those of the second generation, and (J) is that of the third generation. Focused into (H), there are two paths to create (H); ( $\alpha \rightarrow \epsilon$ ) and ( $\gamma \rightarrow \zeta$ ). It can be said that (H) is created from (A) and (C) by multi-path; one is by way of (D) and the other is by way of (E).

## 5. Summary

In summary, by using a 64-channel poloidal Langmuir probe array, the 2D (poloidal mode number  $m$  and frequency  $f$ ) power spectrum of the ion saturation-current fluctuation was measured. 2D bi-coherence analysis, which considers not only the matching condition of  $f$  but also the matching condition of  $m$ , was applied for the observed fluctuation peaks, and the existence of the nonlinear mode couplings among the fluctuation peaks was confirmed. The energy transfer directions among the fluctuation peaks were estimated by amplitude correlation technique. Thus, three original parent modes were found out to be  $(m, f) = (1, 2.8 \text{ kHz})$ ,  $(2, 3.2 \text{ kHz})$  and  $(1, -0.9 \text{ kHz})$ . Other fluctuation peaks were quasi-modes, which were generated successively by mode couplings from the three

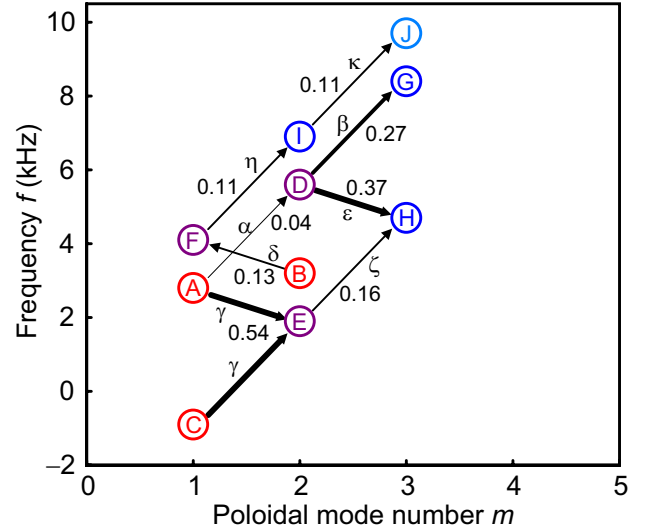


Fig. 5 A chart that shows successive generation of quasi-modes from the three original parent modes (A, B, C). Arrows go from the parent mode to the child mode. The arrows from (A) and (C) are omitted except the cases of  $\alpha$  and  $\gamma$ . The value near the arrow is squared bi-coherence of each mode coupling.

original parent modes. A situation was observed that a quasi-mode of the second generation was created by multi-path.

## Acknowledgments

This work was supported by a Grant-in-Aid for Specially-Promoted Research of MEXT (16002005) (Itoh Project), Grant-in-Aid for Young Scientists (B) of JSPS (19760597), the collaboration programs of NIFS (NIFS07KOAP017) and RIAM, Kyushu University, and Asada Eiichi Research Foundation.

- [1] P.H. Diamond *et al.*, Plasma Phys. Control. Fusion **47**, R35 (2005).
- [2] A. Latten *et al.*, Rev. Sci. Instrum. **66**, 3254 (1995).
- [3] T. Klinger *et al.*, Phys. Rev. Lett. **79**, 3913 (1997).
- [4] N. Krause *et al.*, Rev. Sci. Instrum. **73**, 3474 (2002).
- [5] U. Stroth *et al.*, Phys. Plasmas **11**, 2558 (2004).
- [6] Y.C. Kim and E.J. Powers, Phys. Fluids **21**, 1452 (1978).
- [7] Y. Nagashima *et al.*, Phys. Rev. Lett. **95**, 095002 (2005).
- [8] A. Fujisawa *et al.*, Phys. Rev. Lett. **93**, 165002 (2004).
- [9] T. Yamada *et al.*, Nature Phys. **4**, 721 (2008).
- [10] K. Terasaka *et al.*, Plasma Fusion Res. **2**, 031 (2007).
- [11] T. Yamada *et al.*, Plasma Fusion Res. **3**, 044 (2008).
- [12] T. Yamada *et al.*, Plasma Fusion Res. **3**, S1021 (2008).
- [13] T. Yamada *et al.*, Rev. Sci. Instrum. **78**, 123501 (2007).
- [14] T. Yamada *et al.*, Plasma Fusion Res. **2**, 051 (2007).
- [15] B.B. Kadomtsev, *Plasma Turbulence* (Academic Press, London, 1965) p. 53.
- [16] F.J. Crossley *et al.*, Plasma Phys. Control. Fusion **34**, 235 (1992).
- [17] H. Xia and M.G. Shats, Phys. Rev. Lett. **91**, 155001 (2003).